An Isogeometric Boundary Element Formulation for fibre-reinforced 3D domains

Antonio R. Neto[1], Edson D. Leonel[1]

[1]*Department of Structural Engineering, São Carlos School of Engineering, University of São Paulo*
Av. Trab. São Carlense, 400 - Parque Arnold Schimidt, 13566-590, São Carlos - SP, Brazil
antonio.rodrigues.neto@usp.br, edleonel@sc.usp.br

Abstract. This study presents an innovative Isogeometric coupling formulation for the mechanical analysis of 3D solids reinforced by fibres. This formulation is based on the coupling of the Isogeometric Boundary Element Method (IGABEM) and the 1D approach of the Boundary Element Method (1DBEM). The material matrix (solid 3D domain) is modelled by the IGABEM, which uses NURBS and B-Splines functions to represent both geometry and mechanical fields. These functions allow the exact representation of complex geometries, such as cylinders, torus and propellers. Besides, a straightforward connection with the geometry design is possible, since most CAD packages used in engineering projects represent 3D solids through NURBS surfaces at its contours. The 1DBEM is based on the axial fundamental solution for elastic 1D domains. The interaction between the matrix and fibres is described by an adherence force over the reinforcements' line, which is interpolated by high-order polynomial functions. No relative displacements is considered (perfect bonding) and both materials have linear-elastic behaviour. The proposed coupling formulation is herein named 1DBEM/IGABEM coupling technique. The mechanical analysis of a numerical application demonstrates the results obtained by the proposed formulation in comparison with reference results. The proposed formulation requires fewer degrees of freedom than the reference for the same level of accuracy. Therefore, the Isogeometric coupling presented herein is not only effective for a large number of complex geometries, but also efficient in the precise representation of mechanical fields.

Keywords: 3D IGABEM, Reinforced materials, Coupling formulation.

1 Introduction

Computational mechanics is an essential tool for engineering projects in the prediction of mechanical and structural behaviour. Specially in the context of complex engineering components, such as fibre-reinforced material components of complex geometry, in which experimental testing is expensive and cumbersome. The Isogeometric approach in computational mechanics stand out as a relevant topic in this field, since it enables the exact representation of various complex shapes and the straightforward connection with CAD packages. The IGABEM [1], particularly, best fulfils the isogeometric paradigm due to the non-requirement of domain mesh.

Within this panorama, this study proposes an innovative Isogeometric approach for modelling fibre-reinforced solids using the 3D IGABEM. The consideration of fibres and inclusions in the IGABEM has already been seen in the literature [2], however in a more simple and limited approach. In this study, cracked solids can be represented by the Dual approach [3] and the crossing between fibres and crack faces is possible via 1DBEM connection elements [4].

2 1DBEM/IGABEM Coupling formulation

2.1 3D IGABEM formulation for homogeneous domains

The 3D IGABEM formulation represents the mechanical behaviour of a 3D solid Ω with contour Γ by applying the displacements integral equation (DBIE) into the boundary Γ, which is represented by untrimmed NURBS

surfaces. The DBIE can be obtained through the weighted residual technique, as presented by Brebbia [5], and it is written as follows:

$$c_{ij}(\mathbf{x}^s)u_j(\mathbf{x}^s) + \int_\Gamma T^*_{ij}(\mathbf{x}^s,\mathbf{x}^f)u_j(\mathbf{x}^f)d\Gamma = \int_\Gamma U^*_{ij}(\mathbf{x}^s,\mathbf{x}^f)t_j(\mathbf{x}^f)d\Gamma + \int_\Omega U^*_{ki}(\mathbf{x}^s,\mathbf{x})b_i(\mathbf{x})d\Omega \tag{1}$$

in which $\mathbf{x}^s$ and $\mathbf{x}^f$ indicate the source and field points, respectively. u_j and t_j are boundary displacements and tractions. $c_{ij}(\mathbf{x}^s)$ is the jump term, which equals δ_{ij} if $\mathbf{x}^s$ is an internal point or $\delta_{ij}/2$ if $\mathbf{x}^s$ is positioned in a smooth boundary. δ_{ij} is the Kronecker delta function. U^*_{ij} and T^*_{ij} are the displacements and tractions Kelvin fundamental solutions for 3D domains, respectively, which can be found in Brebbia and Dominguez [5].

The IGABEM solves Eq. 1 in approximate form by discrediting Γ into boundary elements. These elements are represented herein by untrimmed surfaces of Non-Uniform Rational B-Splines (NURBS) functions. Such surfaces are obtained through a tensor product between two uni-variate NURBS curves, which present Basis Functions $N_{i,p}(\xi)$ as follows:

$$\begin{aligned} N_{i,p}(\xi) &= \frac{\xi-\xi_i}{\xi_{i+p}-\xi_i}N_{i,p-1}(\xi) + \frac{\xi_{i+p+1}-\xi}{\xi_{i+p+1}-\xi_{i+1}}N_{i+1,p-1}(\xi) \\ N_{i,0} &= \begin{cases} 1 & \xi_i \leq \xi < \xi_{i+1} \\ 0 & \text{otherwise} \end{cases} \end{aligned} \tag{2}$$

where p is the degree and ξ is the independent parametric coordinate, which has its space delimited by the knot vector $\boldsymbol{\Xi} = \{\xi_1, \xi_2, ..., \xi_t\}$. The subspace between two subsequent knots $[\xi_i, \xi_{i+1}[$ is called knot span.

Then, an untrimmed NURBS surfaces $S_{ij,pq}$ and its Non-Uniform Rational Basis Function $R_{ij,pq}$ can be defined by:

$$\begin{aligned} S_{ij,pq}(\xi,\eta) &= \sum_{i=1}^{n}\sum_{j=1}^{m} R_{ij,pq}(\xi,\eta)B_{ij} \\ R_{ij,pq}(\xi,\eta) &= \frac{N_{i,p}(\xi)M_{j,q}(\eta)w_{ij}}{\sum_{k=1}^{n}\sum_{l=1}^{m} N_{k,p}(\xi)M_{l,q}(\eta)w_{kl}} \end{aligned} \tag{3}$$

in which w_{ij} is the weight associated to the control point B_{ij}. The NURBS surface has two parametric directions ξ and η referent to each uni-variate NURBS curve of degrees p and p, total of control points n and m, Basis Functions $N_{i,p}(\xi)$ and $M_{i,p}(\xi)$ and knot vectors $\boldsymbol{\Xi}$ and $\mathfrak{N}$, respectively.

Thus, $R_{ij,pq}$ approximates both mechanical fields and geometry in a given NURBS surface e as follows:

$$\begin{aligned} \mathbf{u}^e(\xi,\eta) &= \sum_{i=1}^{n}\sum_{j=1}^{m} R_{ij,pq}(\xi,\eta)\hat{\mathbf{u}}^e_{ij} \\ \mathbf{t}^e(\xi,\eta) &= \sum_{i=1}^{n}\sum_{j=1}^{m} R_{ij,pq}(\xi,\eta)\hat{\mathbf{t}}^e_{ij} \end{aligned} \tag{4}$$

in which the displacements and tractions parameters $\hat{\mathbf{u}}$ and $\hat{\mathbf{t}}$, respectively, do not have physical meaning.

The collocation strategy known as Greville Abscissae [6] is applied herein to obtain the collocation points position from the control points positions. For edges with geometric and mechanical field's discontinuities, Cordeiro and Leonel [7] proposed a modification in the collocation strategy to account for discontinuous NURBS.

Then, the fundamental solutions' integration in IGABEM considers the knot spans $[\xi_i, \xi_{i+1}] \times [\eta_i, \eta_{i+1}]$ as "elements". Such parametric local space is converted into Gaussian spaces $[-1,1] \times [-1,1]$, so that numerical Gaussian integration techniques can be applied. The fundamental kernels become singular when integrating the element that contains $\mathbf{x}^s$. In fact, U_{ij} has a weak singularity of order $O(1/r)$ and T_{ij} has a strong singularity of $O(1/r^2)$. To regularise these terms, the integration in polar coordinates is applied for U_{ij} and the singularity subtraction technique proposed by Guiggiani [8] is applied for T_{ij}. Otherwise, the numerical integration may be carried out by standard Gauss-Legendre quadrature. More details about the integration schemes in 3D IGABEM and the analytical expressions provided by the singularity subtraction technique in such case are available in [7].

After applying the discretization technique, Eq. 1 can be algebraically written as follows:

$$\mathbf{H}\hat{\mathbf{u}} = \mathbf{G}\hat{\mathbf{t}} + \int_\Omega U^*_{ki}(\mathbf{x}^s,\mathbf{x})b_i(\mathbf{x})d\Omega \tag{5}$$

where the matrices $\mathbf{H}$ and $\mathbf{G}$ contain, respectively, the integration of kernels T^*_{ij} and U^*_{ij} along Γ. $\hat{\mathbf{u}}$ and $\hat{\mathbf{t}}$ vectors contain, respectively, the global displacement and traction parameters at the control points. The domain integral term will be properly handled in the following sections.

Equation 1 may also represent internal points' displacements, which is algebraically written as:

$$\mathbf{u_i} + \mathbf{H}\hat{\mathbf{u}} = \mathbf{G}\hat{\mathbf{t}} + \int_\Omega U^*_{ki}(\mathbf{x}^i, \mathbf{x}) b_i(\mathbf{x}) d\Omega \tag{6}$$

2.2 Crack modelling in the 3D IGABEM: Dual BEM

The Dual BEM strategy enables the representation of cracks by discretising both faces (denoted by Γ^+_f and Γ^-_f) with coincident NURBS surfaces. Then, the DBIE is applied for collocation points at Γ^+_f and the Tractions integral equation (TBIE) is applied for collocation points at Γ^-_f. Thus:

$$\begin{aligned} &c_{ij}(\mathbf{x}^+)u_j(\mathbf{x}^+) + c_{ij}(\mathbf{x}^-)u_j(\mathbf{x}^-) + \int_\Gamma T^*_{ij}u_j(\mathbf{x}^f)d\Gamma = \int_\Gamma U^*_{ij}t_j(\mathbf{x}^f)d\Gamma + \int_\Omega U^*_{ki}b_i d\Omega \\ &\frac{1}{2}t_j(\mathbf{x}^-) + \frac{1}{2}t_j(\mathbf{x}^+) + \eta_i(\mathbf{x}^-)\int_\Gamma S^*_{kij}u_k(\mathbf{x}^f)d\Gamma = \eta_i(\mathbf{x}^-)\int_\Gamma D^*_{kij}t_k(\mathbf{x}^f)d\Gamma + \eta_i(\mathbf{x}^-)\int_\Gamma D^*_{kij}b_k d\Gamma \end{aligned} \tag{7}$$

where S^*_{kij} and D^*_{kij} are the higher order fundamental solutions, which can be found in the literature [5].

The IGABEM algebraic representation is achieve by combining Eq. 1 for boundary collocation points and Eq. 7 for the crack faces. Such algebraic representation can be written in the same form of Equations 5 and 6.

2.3 Fibres modelling: 1DBEM

The 1DBEM displacements integral equation can also be obtained through the weighted residual technique applied for 1D domains ($\bar{x}$), as described in Neto and Leonel [4] as follows:

$$u_i - N^*_{i1}u_1 + N^*_{in}u_n = -u^*_{i1}N_1 + u^*_{in}N_n + \int_0^L \phi_j(\bar{x})\, u^*_{i\bar{x}}\, d\bar{x}\; p_j \tag{8}$$

in which subscripts 1 and n represent the fibre's endpoints. u_i and N_i are, respectively, the axial displacement and internal force at the i point. ϕ_j are the Lagrangian polynomial functions that approximate the distribuited load over the domain $\bar{x}$ by its nodal values p_i. u^*_{ij} and N^*_{ij} are the fundamental solutions for axial displacements and internal forces, respectively [9].

The integral formulation (Eq. 8) requires boundary discretisation. In such case, the boundary is composed only of the 1D element endpoints, i.e., $i = 1$ and $i = n$. Any other value for i leads to an internal point equation. However, it is interesting to account for internal points equations into the 1DBEM algebraic system, in order to improve the accuracy of the distributed load representation. Besides, the 1DBEM formulation would enable high-order isoparametric elements. Thus, after applying such approximations, Eq. 8 can be algebraically written as follows:

$$\bar{\mathbf{H}}\mathbf{u} = \bar{\mathbf{G}}\mathbf{n} + \bar{\bar{\mathbf{G}}}\mathbf{p} \tag{9}$$

where $\bar{\mathbf{H}}$ and $\bar{\mathbf{G}}$ contain the values of the fundamental solutions N^*_{sf} and u^*_{sf}, respectively, applied in the boundary points. $\mathbf{u}$, $\mathbf{p}$ and $\mathbf{n}$ vectors contain, respectively, the nodal values of axial displacement, nodal values of distributed force and concentrated loads. This expression is so far valid for the local coordinate system. The following global expression can be written by applying axial rotation and considering $\mathbf{n} = \mathbf{0}$:

$$\mathbf{K_F u_F} = \mathbf{G_F p_F} \tag{10}$$

in which $\mathbf{u_F}$ and $\mathbf{p_F}$ vectors contain the values of $\mathbf{u}$ and $\mathbf{p}$ in the global coordinate system.

2.4 Coupling technique

The reinforcements are completely embedded into the solid Ω and positioned along a line $\bar{\Gamma}$, as illustrated in Fig. 1(a). The coupling scheme considers the mechanical interaction among reinforcements and domain as an adherence force, illustrated in Fig. 1(b).

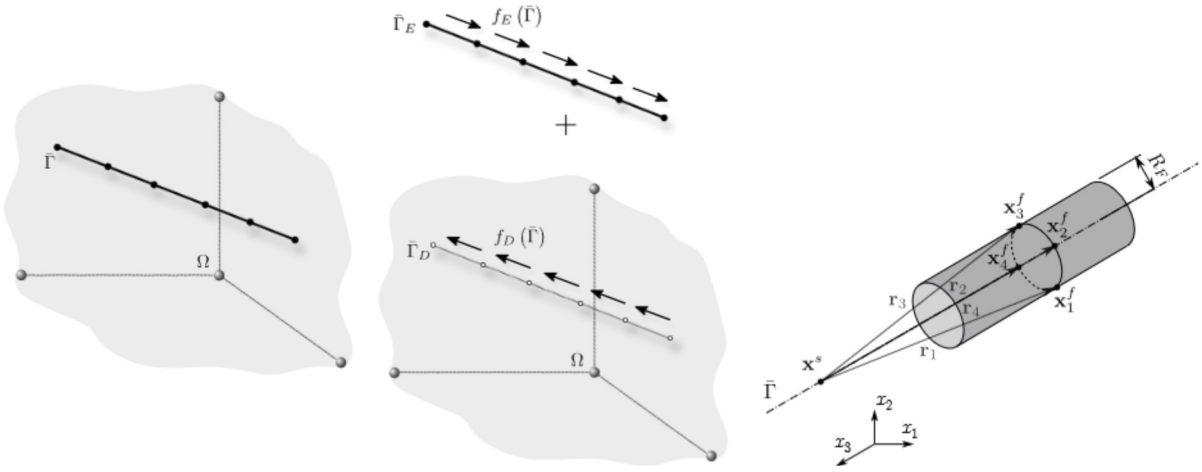

(a) Embedded fibres (b) Mechanical interaction between domain and reinforcement (c) Integration scheme considering 4 angular integration points and a fixed axial coordinate

Figure 1. Scheme of domain/reinforcement coupling technique an fibre integration.

The adherence force is modelled as one-dimensional distributed load along the reinforcement's line $\bar{\Gamma}$. However, one-dimensional loads applied in a three dimensional domain require a special integration scheme, as proposed by Coda et al. [10]. In such scheme, the adherence force is assumed to be applied over a two-dimensional surface and denoted by $\mathbf{Q_i}$. The surface of integration is adopted as a cylindrical shell of radius R_F. Considering the reinforcements as thin elements (length higher than R_F), $\mathbf{Q_i}$ can be simplified as $\mathbf{p_D} = 2\pi R_F \mathbf{Q_i}$.

Thus, the integration of the adherence force over the reinforcements elements can be accounted in the domain term of Eq. 1 and numerically evaluated as follows:

$$\int_{\Omega} U^*_{ki}(\mathbf{x}^s, \mathbf{x}) b_i(\mathbf{x}) d\Omega = \int_{\bar{\Gamma}} U^*_{ij}(\mathbf{p_D})_j d\Gamma = \sum_{g_1=1}^{np_1} \left[\sum_{g_2=1}^{np_2} \left[U_{ij}\left(\mathbf{x}^f(\xi_{g_1}, \xi_{g_2}), \mathbf{x}^s\right) |\mathbf{jac_2}(\xi_{g_2})| \, \omega_{g_2} \right] |\mathbf{jac_1}(\xi_{g_1})| \, \omega_{g_1} \phi_m(\xi_{g_1}) \right] \frac{(\mathbf{p_D})_j}{2\pi R_F} \tag{11}$$

where g_1 and g_2 represent the numerical integrations used for the axial coordinate ($\bar{x}$) and the angular coordinate (θ), respectively. ξ_i, ω_{g_i} and np_i are the dimensionless coordinates, weight values and total number of integration points of the numerical integration i, respectively. Figure 1(c) illustrates the integration over a reinforcement element considering a source point positioned at $\bar{\Gamma}$, considering $np_2 = 4$ and a fixed coordinate ξ_{g_1}.

Therefore, the adherence force can be properly accounted as a body force into the IGABEM formulation through Eq. 11. Hence, the BEM integral equation for boundary points (Eq. 5) can be rewritten as follows:

$$\mathbf{H_{CC}\hat{u}_C} = \mathbf{G_{CC}\hat{t}_C} + \mathbf{G_{CF}p_D} \tag{12}$$

where the term $\mathbf{G_{CF}p_D}$ is the algebraic form of the domain term obtained by applying Eq. 11. In the above equation, the subscripts of the matrices $\mathbf{H}$ and $\mathbf{F}$ represent the position of source and field points, being at the boundary ($\mathbf{C}$) or at the fibres ($\mathbf{F}$).

The IGABEM integral equation for internal points (Eq. 6) can also be rewritten herein. This equation must be applied for internal points coincident with the reinforcements nodes, i.e., $\mathbf{u_i} = \mathbf{u_D}$. Thus:

$$\mathbf{u_D} = \mathbf{G_{FC}\hat{t}_C} - \mathbf{H_{FC}\hat{u}_C} + \mathbf{G_{FF}p_D} \tag{13}$$

The proposed model assumes perfect bond conditions among reinforcements and domain. Then, the compatibility of displacements and equilibrium of forces are enforced among reinforcements and domain as follows:

$$\mathbf{u_F} = \mathbf{u_D} \qquad \text{and} \qquad \mathbf{p_F} = -\mathbf{p_D} \tag{14}$$

The resulting algebraic system of equations is then obtained by coupling Eq. 12, Eq. 13 and Eq. 9. In addition, the application of the compatibility relations from Eq. 14 leads to:

$$\begin{bmatrix} \mathbf{H_{CC}} & \mathbf{0} & -\mathbf{G_{CF}} \\ \mathbf{H_{FC}} & \mathbf{I} & -\mathbf{G_{FF}} \\ \mathbf{0} & \mathbf{K_F} & \mathbf{G_F} \end{bmatrix} \begin{Bmatrix} \hat{\mathbf{u}}_\mathbf{C} \\ \mathbf{u_D} \\ \mathbf{p_D} \end{Bmatrix} = \begin{bmatrix} \mathbf{G_{CC}} \\ \mathbf{G_{FC}} \\ \mathbf{0} \end{bmatrix} \{\hat{\mathbf{t}}_\mathbf{C}\} \tag{15}$$

where $\mathbf{I}$ is the identity matrix. The last equation is solved by enforcing the boundary conditions by moving the known values of $\hat{\mathbf{t}}_\mathbf{C}$ to the right-hand side and the unknown ones to the left-hand side.

3 Numerical results

This numerical example consists of a solid with a single edge notch reinforced by four long fibres, as illustrated in Fig. 2(a). The physical properties are: $h = 10$ cm, $b = 5$ cm, $a = 2.5$ cm and $\sigma = 1$ kN/cm^2. The solid's material presents: Young's modulus $E = 1000$ kN/cm^2 and Poisson's ratio $\nu = 0.2$. The fibres have circular cross-section with radius $r = 0.2$ cm and three different values of Young's modulus are considered: $E_0 = 0$, $E_{500} = 500$, $E_{1000} = 1000$ and $E_{1500} = 1500$ kN/cm^2.

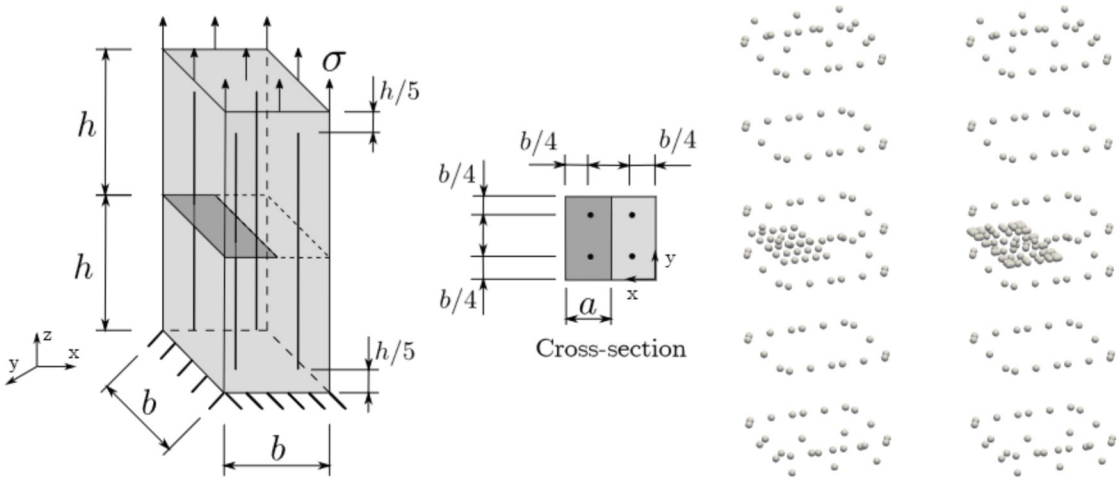

(a) Structure (b) Mesh A (c) Mesh B

Figure 2. Reinforced cracked solid analysed with IGABEM coupling formulation and Isogeometric boundary meshes (collocation points).

Two isogeometric meshes are used to represent the solid. Both of them are composed by 14 bi-quadratic ($p = q = 2$) regular NURBS surfaces for the external boundaries and 2 regular NURBS surfaces of $p = q = 4$ that represent the crack faces. Mesh A is applied in the mechanical analyses without fibres (scenario $E_F = 0$) and presents all NURBS surfaces with only one knot span, which results in 176 collocation points. Mesh B is derived from Mesh A by refining the crack surfaces with 3 knot insertions [11], which results in 254 collocation points. The second mesh is applied for the analyses with the presence of fibres, which require thinner discretization of the crack due to its complex mechanical behaviour when affected by the crossing fibres. Figures 2(b) and 2(c) illustrates both meshes. Mesh convergence has been previously verified regarding displacements at the boundary.

The fibres discretisation is the same in all of the scenarios. Each one of the four long fibres is represented by 16 quadratic elements, which leads to a total of 134 collocation points. The crossing between the fibres and the crack is represented by the connection element strategy, presented by Neto and Leonel [4].

Reference results are found in the literature [12] for a 2D equivalent problem without the fibres. The results are presented as the crack mouth opening displacement (CMOD) values, which can be used as reference for the scenario with $E_F = 0$. The CMOD (δ) is:

$$\delta = \left(\frac{4\sigma a}{E'}\right) \frac{1.46 + 3.42\left(1 - \cos\frac{\pi a}{2b}\right)}{\left(\cos\frac{\pi a}{2b}\right)^2} \tag{16}$$

in which $E' = E/(1-\nu^2)$. The reference results are constant along the dimension x of the analysed model, since they come from a 2D equivalent problem.

Figure 3 illustrates the results of CMOD along the crack mouth (direction x) obtained in all of the three scenarios and the reference results (from Eq. 16) labelled as "Analytical". This figure demonstrates that increasing the fibres Young's modulus leads to a decrease in the value of the CMOD, as expected. In fact, all of the scenarios with non-zero fibres Young's modulus are significantly far from the other ones, which is expected since the presence of fibres introduces a material continuity at the crack surface. Provided that this analysis imposes linear behaviour, it surely must drastically affect the crack opening.

It is worth mentioning that the greatest error value between E_0 and the analytical results from Eq. 16 was 0.72%. Thus, the results demonstrate accuracy as far as the reference comparison is valid.

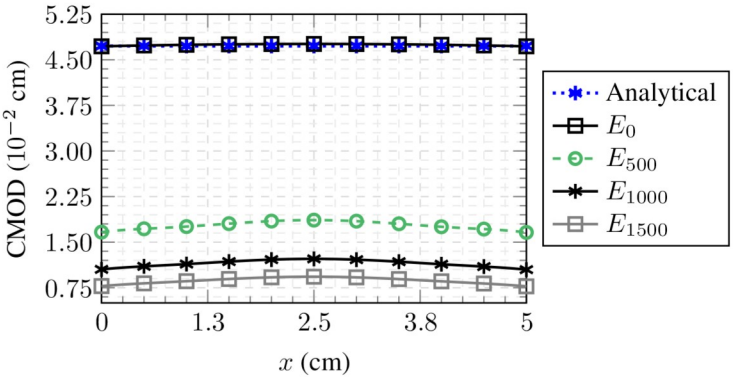

Figure 3. Crack opening displacements along the crack mouth (direction x).

Figure 4 illustrates the z displacements fields over the solid's deformed shape obtained in all of the four scenarios. A scale factor of 50 is considered. The NURBS surfaces are subdivided into 100 auxiliary Lagrangian elements (4-node) to generate the visualisation. This figure demonstrates that the solid's deformed shape is coherent in all of the analyses. Furthermore, one observes the fibres' effect on the crack surface, which presents a slight deformation that reminds a fibre pullout.

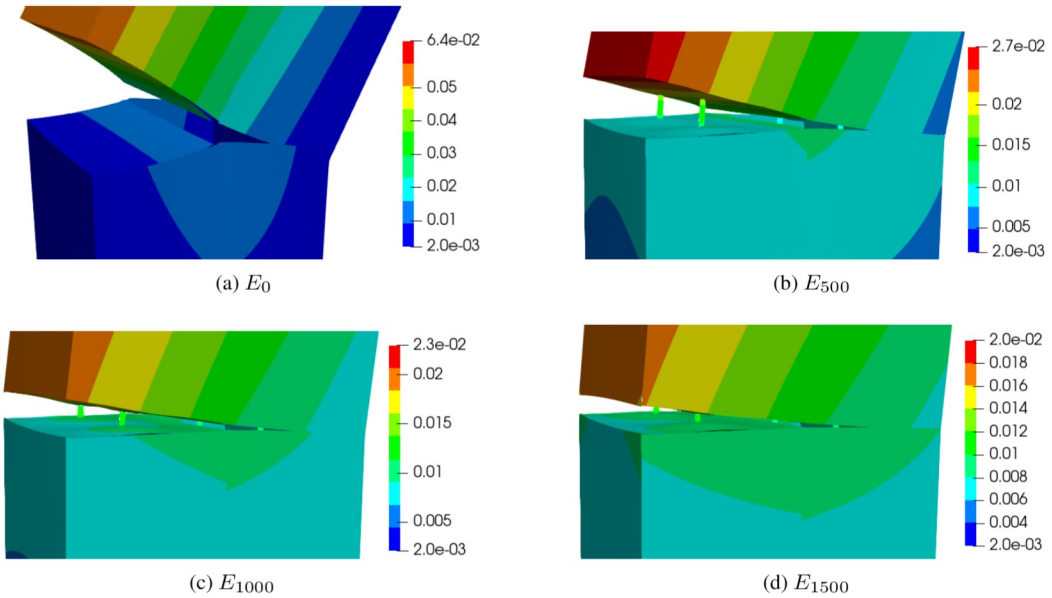

(a) E_0 (b) E_{500}

(c) E_{1000} (d) E_{1500}

Figure 4. Deformed shape and z displacements field obtained via the IGABEM for each scenario. Scale factor equals 50.

Figure 5 presents the axial stress obtained in each scenario along the fibre's length (S_f), considering the fibre that crosses the crack. This figure demonstrates a massive stress concentration in the fibre's region near the crack (around $S = 8$ cm). This behaviour is explained by the fact that the fibres remain linear-elastic. In a real scenario, that region would present both yielding and slipping, which would cause energy dissipation and decrease the stress concentration. Besides, it is worth highlighting that the scenarios with higher fibres Young's modulus show higher values of axial stress.

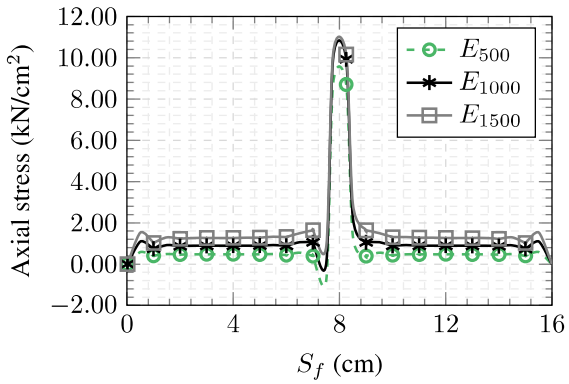

Figure 5. Axial stresses along the fiber that crosses the crack obtained in each reinforced scenario.

4 Conclusions

This study presented an innovative isogeometric approach to model fibre-reinforced solids. The IGABEM has been coupled with the 1DBEM and the Dual BEM formulation has been applied to represent cracked bodies. The numerical application has shown the good results obtained by the proposed formulation. In the context of fibre-reinforced cracked bodies, material nonlinearities have a significant contribution, thus this matter stands out as a proposed future development.

Acknowledgements. Sponsorship of this research project by the São Paulo State Foundation for Research (FAPESP), project number 2018/20253-4, is greatly appreciated.

Authorship statement. The authors hereby confirm that they are the sole liable persons responsible for the authorship of this work, and that all material that has been herein included as part of the present paper is either the property (and authorship) of the authors, or has the permission of the owners to be included here.

References

[1] R. N. Simpson, S. P. Bordas, J. Trevelyan, and T. Rabczuk. A two-dimensional isogeometric boundary element method for elastostatic analysis. *Computer Methods in Applied Mechanics and Engineering*, vol. 209, pp. 87–100, 2012.

[2] G. Beer, C. Dünser, E. Ruocco, and V. Mallardo. Efficient simulation of inclusions and reinforcement bars with the isogeometric boundary element method. *Computer Methods in Applied Mechanics and Engineering*, vol. 372, pp. 113409, 2020.

[3] H.-K. Hong and J.-T. Chen. Derivations of integral equations of elasticity. *Journal of Engineering Mechanics*, vol. 114, n. 6, pp. 1028–1044, 1988.

[4] A. R. Neto and E. D. Leonel. Three dimensional nonlinear BEM formulations for the mechanical analysis of nonhomogeneous reinforced structural systems. *Engineering Analysis with Boundary Elements*, vol. 123, pp. 200 – 219, 2021.

[5] C. A. Brebbia. Weighted residual classification of approximate methods. *Applied Mathematical Modelling*, vol. 2, n. 3, pp. 160 – 164, 1978.

[6] T. Greville. Numerical procedures for interpolation by spline functions. *Journal of the Society for Industrial and Applied Mathematics, Series B: Numerical Analysis*, vol. 1, n. 1, pp. 53–68, 1964.

[7] S. G. F. Cordeiro and E. D. Leonel. Mechanical modelling of three-dimensional cracked structural components using the isogeometric dual boundary element method. *Applied Mathematical Modelling*, vol. 63, pp. 415–444, 2018.

[8] M. Guiggiani and A. Gigante. A General Algorithm for Multidimensional Cauchy Principal Value Integrals in the Boundary Element Method. *Journal of Applied Mechanics*, vol. 57, n. 4, pp. 906–915, 1990.

[9] P. K. Banerjee and R. Butterfield. *Boundary element methods in engineering science*, volume 17. McGraw-Hill, London, 1981.

[10] H. B. Coda, W. S. Venturini, and M. H. Aliabadi. A general 3D BEM/FEM coupling applied to elastodynamic continua/frame structures interaction analysis. *International Journal for Numerical Methods in Engineering*, vol. 46, n. 5, pp. 695–712, 1999.

[11] L. Piegl and W. Tiller. *The NURBS book*. Springer Science & Business Media, 2012.

[12] H. Tada, P. Paris, and G. Irwin. The analysis of cracks handbook. *New York: ASME Press*, vol. 2, pp. 1, 2000.